PROCEEDINGS OF THE ROYAL SOCIETY A MATHEMATICAL, PHYSICAL & ENGINEERING SCIENCES

An Experimental Study of High-Pressure Bubble Growth Within Multicomponent Liquid Droplets Levitated in a Flowing Stream of Another Immiscible Liquid

C. T. Avedisian

Proc. R. Soc. Lond. A 1987 **409**, doi: 10.1098/rspa.1987.0017, published 9 February 1987

Proc. R. Soc. Lond. A **409**, 271–285 (1987)
Printed in Great Britain

An experimental study of high-pressure bubble growth within multicomponent liquid droplets levitated in a flowing stream of another immiscible liquid

By C. T. Avedisian

Sibley School of Mechanical and Aerospace Engineering, Cornell University, Ithaca, New York 14853, *U.S.A.*

(*Communicated by M. E. Fisher, F.R.S. – Received* 13 *December* 1985 *– Revised* 2 *April* 1986)

Measurements of vaporization rates of highly superheated liquid droplets are reported at reduced pressures up to 0.4 and reduced temperatures up to 0.95. Binary and ternary mixtures of *n*-pentane, *n*-hexane, and *n*-decane, were studied. The experimental method involved levitating a test droplet in a flowing stream of another immiscible liquid (glycerine). Levitation was achieved by balancing the buoyancy and drag force on the droplet. Bubble formation within the droplet was induced by isothermally decompressing the field liquid to pressures approaching the homogeneous nucleation limit of the levitated droplet.

It was observed that a droplet consisting of a binary *n*-pentane–*n*-hexane mixture vaporized faster than either an *n*-pentane or *n*-hexane droplet, and that the vaporization rate decreased with increasing pressure. Replacing part of the non-volatile component of a *n*-pentane–*n*-hexane mixture by a yet more non-volatile liquid (*n*-decane), thus forming a ternary pentane–hexane–decane mixture, was found to increase the vaporization rate above that of a droplet consisting of a binary mixture of the most volatile component with any one of the other two components. The results are discussed from the perspective of bubble growth within a liquid mixture of infinite extent.

1. Introduction

The dynamics of phase change of a liquid in the metastable state is a two-step process, involving bubble nucleation and bubble growth. The first process provides no information about the second, though a phase change at the superheat limit is often assumed to be explosive, independent of the far-field pressure or liquid composition. This belief was supported in work reported by Apfel & Harbison (1975) and Mori & Komotori (1976). Subsequent experiments performed by Shepherd & Sturtevant (1982) and Frost & Sturtevant (1986) revealed the dynamic nature of explosive vaporization of pure liquid droplets at the superheat limit. They found explosive vaporization of droplets to be driven by a mass transfer induced instability akin to the Landau instability of flames, and that the process occurred on a microsecond time scale.

The effects of ambient pressure on evaporation of *pure* liquid droplets at the superheat limit have been examined by Avedisian (1982) and Frost & Sturtevant

(1986). It was found that the dynamic instability that drives rapid (i.e. explosive) evaporation at atmospheric pressure was completely eliminated at higher pressures for several organic liquids (butane, pentane, octane and ether) such that the test droplets simply swelled quiescently on a millisecond time scale as the internal bubble grew, rather than exhibiting the characteristics of a wrinkled non-smooth evaporating boundary of an exploding droplet (Frost & Sturtevant 1986). Liquid composition has also been observed to effect the dynamics of bubble growth within droplets, which are binary miscible mixtures of liquids, though the reported observations have only been qualitative (i.e. made with the naked eye (see, for example, Blander *et al.* 1971)).

The present work examines the effects of both ambient pressure and liquid composition on the dynamics of phase change of multicomponent liquid droplets at their homogeneous nucleation limits at high pressures (up to 1.3 MPa). An apparatus was designed to levitate a single, light, test droplet within a flowing stream of another, heavier, immiscible liquid in a vertical pressure cell, and then to induce bubble nucleation within the droplet by isothermally decompressing the field liquid. The chief advantage of this method is in providing isothermal initial conditions within the droplet, and in producing relatively stationary droplets to facilitate photographic documentation of their vaporization.

Levitation was achieved by balancing the drag force around the droplet with its buoyancy force. In this manner the droplet was effectively held motionless during an experiment. Bubble formation was initiated within the droplet by releasing the pressure on the field liquid, while maintaining its temperature constant, to values very close to the homogeneous nucleation limit. High-speed cine photography was used to record both qualitative aspects of the dynamics of phase change at the superheat, and quantitative information on the evolution of droplet diameter as a function of pressure and composition. In view of the elevated pressures of interest in this work, camera framing rates of under 1000 frames s^{-1} were found to be sufficient for recording all stages of phase growth except those under explosive conditions (i.e. for pressures near atmospheric). The test fluids used were *n*-pentane, *n*-hexane, and *n*-decane. Composition of the droplets consisted of two binary and one ternary mixture. The field liquid was glycerine because of its immiscibility with the test liquids and its other favourable properties for driving the potential for nucleation to within the bulk of the droplets rather than at the droplet–field-liquid interface. As such the glycerine served only as a medium to establish the initial temperature and pressure of the droplet and did not otherwise inhibit the ability of the droplets to undergo an intrinsic phase transition.

2. Apparatus and procedure

Figure 1 is a schematic diagram of the apparatus. Primary components are (1) a high-pressure test chamber containing a diffuser section, (2) upper plenum, (3) recirculation loop, (4) droplet injector and (5) photographic instrumentation. The entire circulation loop was designed to withstand pressures up to 2.5 MPa so as to allow droplets to be introduced under static pressures above their bubble-point pressures at the preselected temperatures.

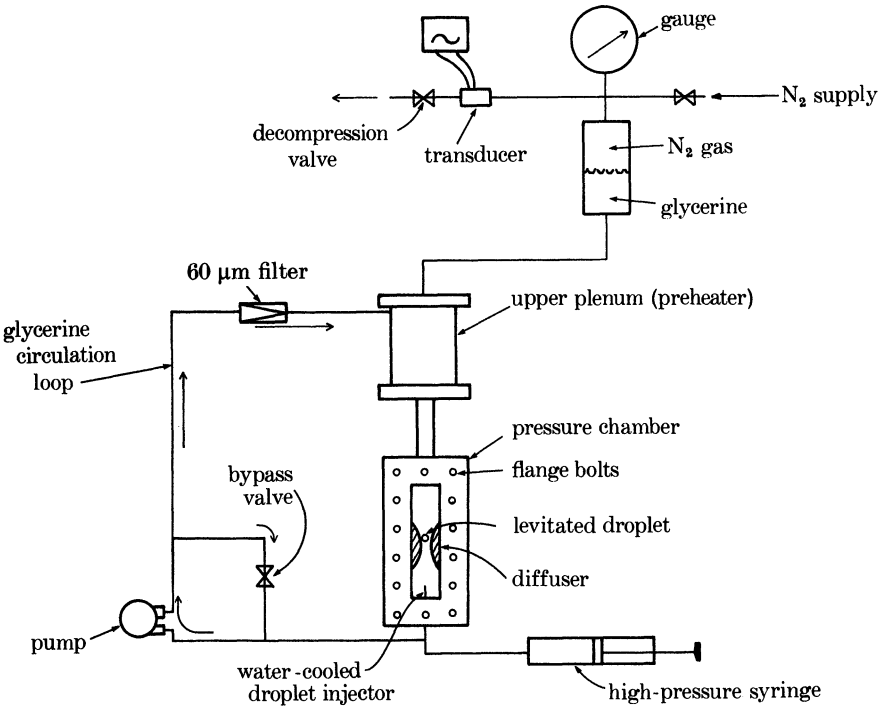

FIGURE 1. Schematic diagram of the apparatus.

The test section consisted of a solid stainless steel block 3.8 cm thick 11.4 cm wide and 34.4 cm long. A rectangular opening, tapered from 2.6 cm wide at the top to 6.4 cm at the bottom, was machined in the centre of the block, providing a diverging channel (angle of 6.3°) for liquid flow into the top. Movable stainless steel side walls (3.2 cm thick) were placed within this diverging section, to which were attached circular segments cut from a solid stainless-steel block 15.2 cm diameter and machined to 6.3 cm in length. These arcs essentially created a converging–diverging diffuser with a nominal spacing of 1.3 cm. Droplets were levitated in this throat section. This arrangement allowed maximum flexibility for varying the throat spacing and diffuser angle. The chamber opening was sealed with flat glass sides, 2.54 cm thick, so as to eliminate any lens effect that would distort the droplet image.

The upper plenum served as a trap for air bubbles introduced in the test section during filling and vaporization, and also as a preheater. The plenum was connected to the test section inlet via a rectangular stainless steel channel, machined to provide a smooth contour with the inlet. The resulting flow was very uniform at the high temperatures studied, with streamlines (observed by impurities and small air bubbles introduced for visualization) parallel to the test section walls and diffuser section.

The droplet injector was a stainless steel tube (0.1 mm in diameter) placed in a water-cooled jacket 0.64 cm diameter 13.3 cm long. The tube was connected to a high-pressure syringe (High Pressure Equipment Co., Erie, Pennsylvania) which

could be manipulated to force single droplets out of the tube. Liquid circulation was achieved via a Model 17AM01 Roper Pump (Commerce, Georgia).

Pressure was measured by a Heise gauge (0–2.5 MPa) calibrated to ± 0.007 MPa. Temperatures were measured with three chromel–alumel thermocouples sheathed by stainless steel (0.16 cm diameter) placed within the test section. Temperatures of these three thermocouples varied by less than 1 K during an experiment.

An experiment was initiated by establishing a uniform flow rate of glycerine at the preselected temperature. The initial pressure was slightly less (a few kilopascals) than the bubble-point pressure of the test droplet corresponding to the field liquid temperature (these pressures ranged between 1.7 and 2.3 MPa for the mixtures studied). The flow rate (corresponding to Peclet numbers, Pe, of about 30 and $U_\infty \approx 1$ cm s^{-1}) could be adjusted with the bypass valve to levitate a droplet just above the throat of the diffuser section. This fine tuning of the flow rate was affected with a constant pump speed. A period of about 2 min was then allowed to elapse before decompressing (at a typical rate of 0.2 MPa s^{-1}) to ensure an isothermal droplet.

The nucleation pressure was accurately measured by recording the droplet vaporization process on video tape (in addition to simultaneously photographing it with a high-speed cine camera). Two video cameras (not shown in figure 1) were used for this purpose: one directed at the pressure gauge and one directed at the droplet. The two images were viewed simultaneously on a split screen monitor, thus permitting an accurate (to ± 0.007 MPa) and simple measurement of the pressure at which vaporization occurred. Table 1 summarizes these data (T_∞, P_0) corresponding to the mixtures for which bubble-growth measurements are reported. Other separate measurements were made exclusively of the incipient nucleation limit to ascertain if the test droplet was at its homogeneous nucleation limit when a bubble formed within it as discussed in §3.1.

High-speed cine photography with a Hycam II camera fitted with a Nikon 105 mm macrolens and direct back lighting was used to document the behaviour of the droplets as they vaporized. Figure 2 illustrates several representative motion

TABLE 1. SUMMARY OF INITIAL CONDITIONS FOR BUBBLE-GROWTH EXPERIMENTS

($C_5 = n$-C_5H_{12} (pentane) $C_6 = n$-C_6H_{14} (hexane) $C_{10} = n$-$C_{10}H_{22}$ (decane))

composition (mole fraction)	drop number	P_0/MPa	T_∞/K	S_0/mm
$1.0C_5$	29	0.75	427.9	0.76
$1.0C_5$	31	1.16	435.3	0.80
$0.715C_5:0.285C_6$	17	0.76	422.3	0.80
$0.715C_5:0.285C_6$	20	1.22	447.7	0.60
$0.456C_5:0.544C_6$	11	0.82	452.0	0.71
$0.456C_5:0.544C_6$	14	1.18	467.7	0.74
$0.219C_5:0.718C_6$	4	0.73	461.2	0.81
$0.219C_5:0.118C_6$	7	1.04	463.9	0.74
$1.0C_6$	40	0.80	468.3	0.78
$1.0C_6$	39	0.82	468.1	0.72
$1.0C_6$	43	1.20	475.3	0.74
$0.8C_5:0.2C_{10}$	34	0.79	471.6	0.70
$0.8C_5:0.1C_6:0.1C_{10}$	47	0.71	454.2	0.77

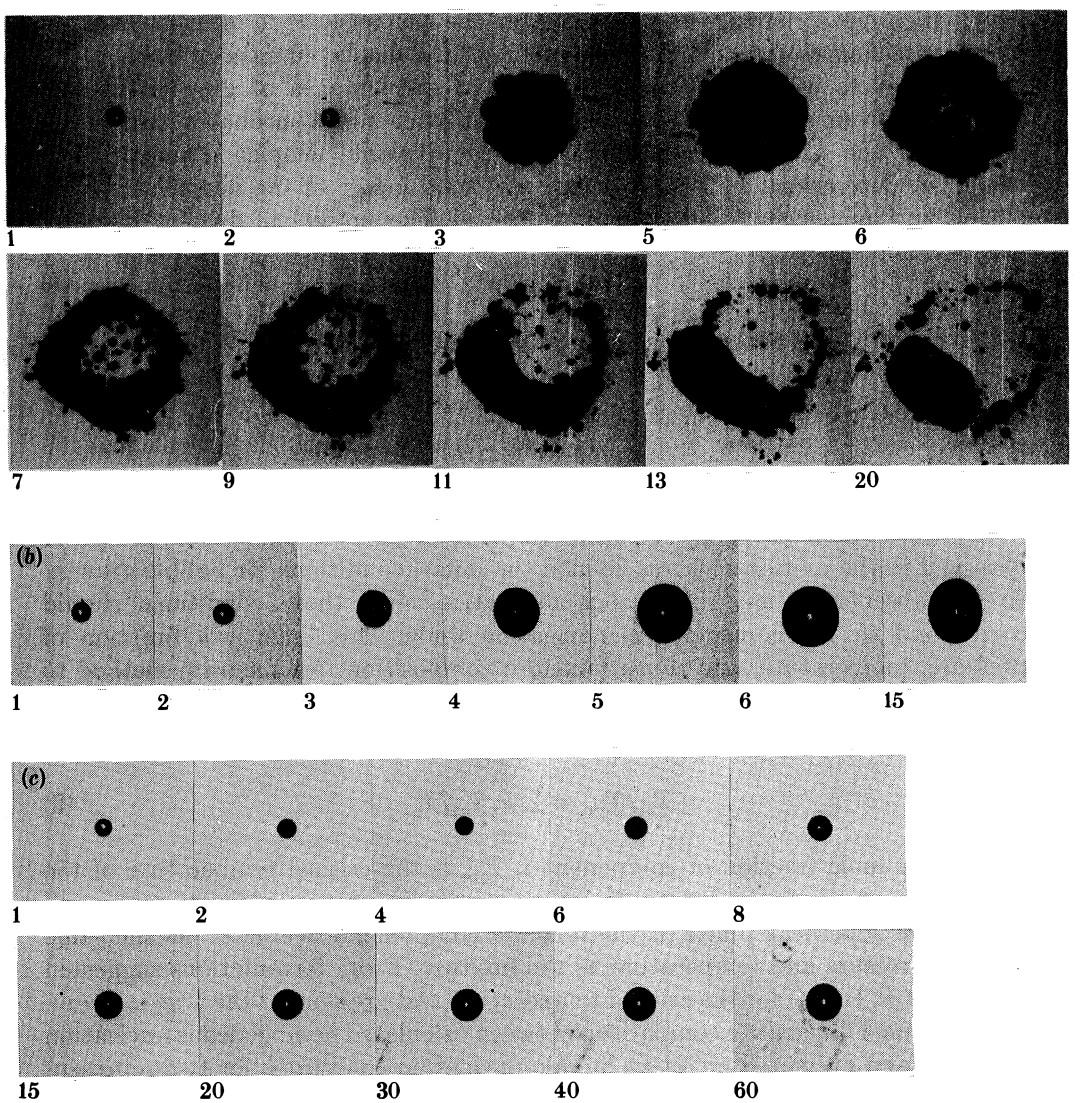

FIGURE 2. Levitated droplets at their superheat limits in glycerine. Flow is from left to right. Number on each picture corresponds to the position in the motion picture sequence. (*a*) *n*-hexane: $P_0 = 0.12$ MPa, $T_\infty = 460$ K, $S_0 = 0.72$ mm, frames $s^{-1} = 900$; (*b*) *n*-hexane: $P_0 = 0.44$ MPa, $T_\infty = 461.3$ K, $S_0 = 0.76$ mm, frames $s^{-1} = 500$; (*c*) *n*-pentane (0.715)–*n*-hexane (0.285) mixture: $P_0 = 0.93$ MPa, $T_\infty = 450$ K, $S_0 = 0.7$ mm, frames $s^{-1} = 500$. White dot in droplet centre is light reflection.

picture sequences, which will be discussed in §3. Framing rates between 500 frames s^{-1} and 1000 frames s^{-1} were found to be sufficiently fast for recording vaporization at all but explosive conditions. Bubble-growth measurements were obtained from a frame-by-frame analysis of these movies. The overall droplet diameter, S, was measured because the internal bubble dimensions could not be clearly observed.

A motion-picture analyser was used to produce an enlarged image of each frame from which measurements were made. Also, the droplet-growth measurements in all relevant figures correspond to the centre of the displayed data symbol.

The droplets were nearly spherical in the early stages of growth, though deviations from sphericity were observed at later times, probably caused by motion of the ambient field liquid. An 'equivalent' droplet diameter was, therefore, determined by assuming the projected image of the droplet to be an ellipse, and its volume to be an oblate spheroid. The equivalent droplet diameter was calculated as

$$S = (ab^2)^{\frac{1}{3}}, \tag{1}$$

where a and b were measured as major and minor droplet axes.

3. Results and discussion

3.1. *Initial conditions for bubble growth*

The initial ambient pressure and temperature at which a bubble was first observed in the motion pictures defined the initial conditions for bubble growth. In the absence of any extraneous nucleation aids, these conditions should correspond to the homogeneous nucleation limit. This limit is a function of pressure, temperature, and (for a mixture) composition. An accurate method to predict the nucleation limit for mixtures has been presented by Avedisian & Sullivan (1984) based on corresponding states.

$$T_\infty/T_{\mathrm{cm}} = \sum x_i T_{\mathrm{n}i}/T_{\mathrm{c}i}, \tag{2}$$

where x_i is mole fraction of component i, T_{cm} is the critical temperature of the composition-dependent mixture, $T_{\mathrm{c}i}$ is the critical temperature of component i, and the $T_{\mathrm{n}i}$ are superheat limits of the mixture components evaluated at the same reduced pressure and temperature as the mixture. From formulations suggested by Reid *et al.* (1977) for the critical temperature and pressure of the true mixture, figures 3 and 4 illustrate a comparison between calculated homogeneous nucleation limits (2) and measured incipient bubble-nucleation conditions for two representative mixtures: a binary *n*-pentane–*n*-hexane mixture at a fixed pressure, 0.76 MPa, but with composition varying, and a ternary *n*-pentane–*n*-hexane–*n*-decane mixture of fixed composition (80 % pentane, 10 % hexane, 10 % decane†) and pressure ranging between 0.54 and 1.6 MPa. Calculated bubble point lines for these mixtures are also shown to illustrate the extent of superheating. These latter calculations were made by using Raoult's Law coupled with the Antoine equations (see, for example, Reid *et al.* 1977) for component vapour pressures. Liquid states between the bubble line and limit of superheat are in principle possible, with the homogeneous nucleation limit (T_∞) imposing the highest possible superheat. Figures 3 and 4 provide evidence to verify that the droplets were initially at this limit before bubble growth commenced.

† All percentage compositions are molar.

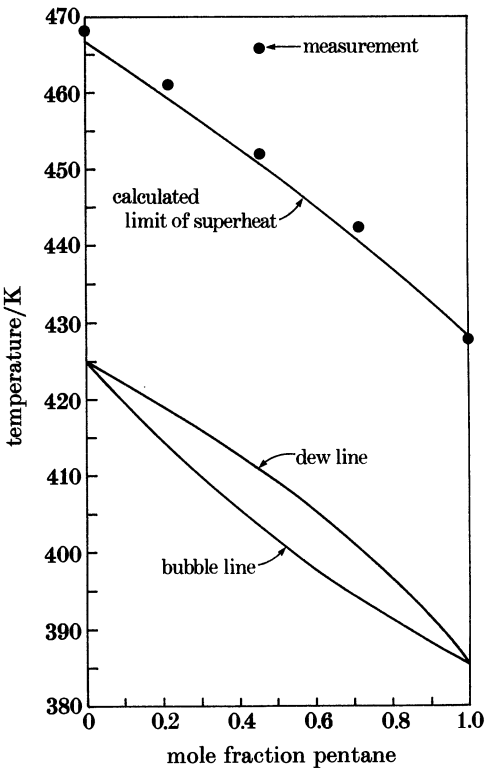

FIGURE 3. Comparison between predicted (T_∞) and measured initial droplet states for bubble nucleation within a pentane–hexane mixture at 0.76 MPa. Prediction is based on the homogeneous nucleation limit (2). The bubble and dew lines for this mixture are also shown.

3.2. *Dynamics of bubble growth*

The limit of superheat provides no information about the dynamics of bubble growth within a droplet. The initial bubble may grow sufficiently rapid that the droplet explodes into vapour, or bubble growth can be quiescent.

Figure 2 shows representative observations of the dynamics of phase change at the superheat limit for pure hexane and a pentane–hexane mixture droplet. Figure 2*a* illustrates a photographic sequence (at 900 frames s^{-1}) of a pure levitated *n*-hexane droplet vaporizing at 0.12 MPa. The flow is from left to right at a velocity of about 1 cm s^{-1} (Reynolds number of about 10). Figure 2*b* illustrates a droplet of nearly the same initial size but at 0.44 MPa. The elimination of explosive vaporization as pressure increases is clearly illustrated in these photographs, yet in both instances the droplet was at its superheat limit. Further increases in ambient pressure led to a continued reduction in the droplet expansion rate. Figure 2*c* shows a 72 % pentane in hexane mixture at 0.93 MPa.

An explanation for the elimination of explosive vaporization of pure liquids with increasing pressure centres around a combination of a Landau-type instability mechanism, which drives rapid evaporation at the superheat limit (Frost &

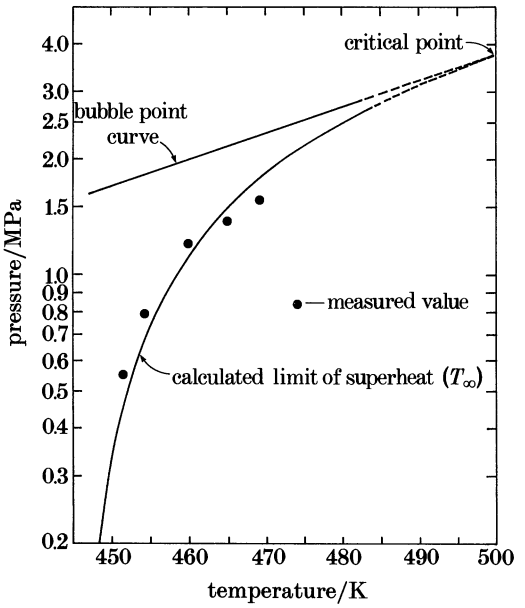

FIGURE 4. Comparison between measured and predicted nucleation pressures for a ternary pentane–hexane–decane mixture containing 80 % pentane, 10 % hexane, and 10 % decane. The bubble point limit represents the initial glycerine pressure at the start of decompression and under which a droplet was introduced into the test section.

Sturtevant 1986), and a reduction of a large initial pressure difference across the liquid–vapour interface of the internal bubble with increasing ambient pressure (Avedisian 1982). With the elimination of such a pressure difference, bubble growth becomes more limited by heat transfer from the ambient liquid. In a mixture, composition also effects the droplet expansion rate as discussed below.

Figure 5 illustrates an example of the repeatability of the droplet diameter measurements. The normalized droplet diameter S/S_0, is plotted against a non-dimensional time $\tau(\tau = t\alpha/S_0^2$, where α is the mixture thermal diffusivity and S_0 is the initial droplet diameter). Data from two different droplets at nearly the same temperature and slightly different pressures are shown: 0.8 and 0.82 MPa. With temperature as the controlled variable and the rather weak variation of superheat limit with pressure (figure 4) it was very difficult to precisely reproduce the nucleation pressure for two different droplets. Nevertheless, the relative placement of the data is consistent with the ordering of pressures. We note that in this and subsequent figures the overall droplet diameter S is displayed, and not the internal bubble diameter d.

Figure 6 shows the variation of droplet diameter for a pentane–hexane mixture at 0.76 MPa. At constant pressure, the droplet expands due to growth of the internal bubble, and growth stops when the droplet reaches a final size corresponding to complete evaporation of the original liquid mass,

$$S_f/S_0 = (1-\epsilon)^{-\frac{1}{3}}, \tag{3}$$

where $\epsilon = 1-\rho_g/\rho_l$ and ρ_g and ρ_l and are vapour and liquid densities, respectively.

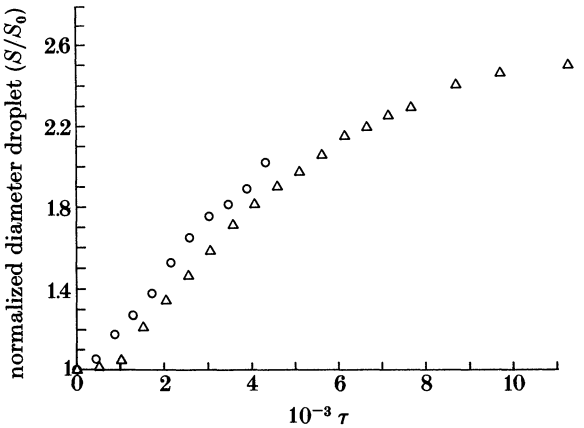

FIGURE 5. Variation of droplet diameter with time for pure *n*-hexane at 0.82 MPa (○, drop 39) and 0.80 MPa (△, drop 40). Results illustrate a measure of the repeatability of the experiments.

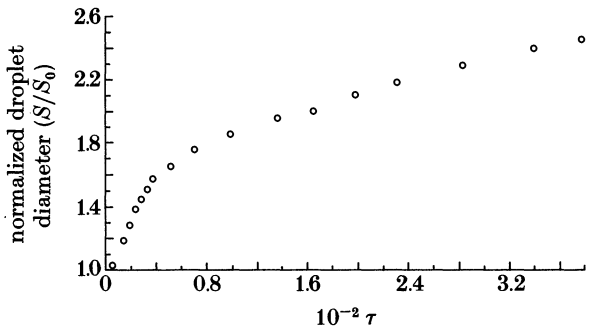

FIGURE 6. Measured variation of droplet diameter (S/S_0) with time (τ) for drop 17.

By contrast, the bubble size for growth in a liquid of infinite extent ($S_0 \to \infty$) is unbounded. For the elevated pressures studied (e.g. figure 2*b*, *c*), droplet oscillations of the type noted by Apfel & Harbison (1975) were not observed. The initial ambient pressure was apparently high enough and the growth rate low enough in our experiments to suppress overshooting the final equilibrium droplet size, a measure of which is given by (3).

The effect of initial ambient pressure on the droplet growth rate is shown in figures 7 and 8 for pure pentane and a pentane–hexane mixture, respectively. In both cases, increasing the ambient pressure was found to have a strong effect on the droplet expansion rate such that this rate (the slope in figures 7 and 8) was reduced by more than 50% for a 65% increase in pressure. This reduction is conjectured to be due to a lowering of the initial excess pressure in the bubble over the ambient pressure as ambient pressure increases as shown, for example, schematically in figure 9 (the saturation curve approximately corresponds to the gas pressure in the bubble).

Whether or not the internal droplet expansion rate is controlled by inertia or

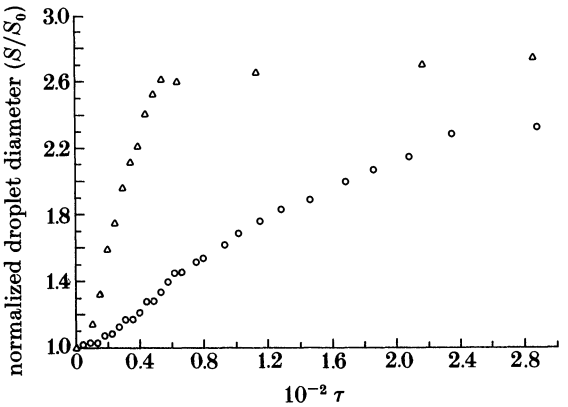

FIGURE 7. Effect of pressure on droplet expansion rate for pure n-pentane at 0.75 MPa (△, drop 29) and 1.16 MPa (○, drop 31).

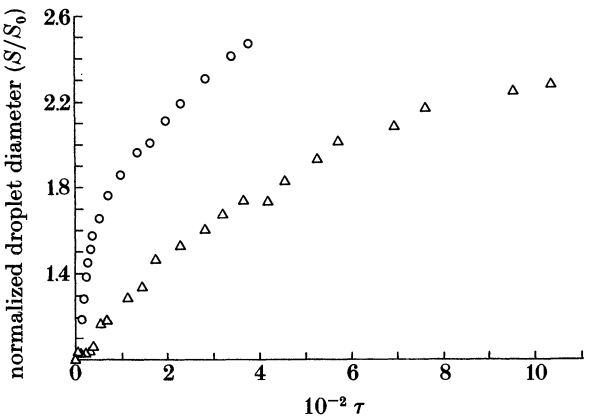

FIGURE 8. Effect of pressure on droplet expansion rate for a binary pentane–hexane mixture at 0.76 MPa (○, drop 17) and 1.22 MPa (△, drop 20).

heat transfer from the surrounding liquid, the initial excess pressure $\Delta P_i \equiv P_v(t=0) - P_0$ provides a measure of the growth rate, where $P_v(t=0)$ is the vapour pressure in the critical size nucleus and P_0 is the ambient liquid pressure (see figure 9). For isothermal (i.e. inertia-limited) growth, an increase in P_0 results in a decrease of ΔP_i because $\Delta P_i \to 0$ as $P_0 \to P_c$ (critical pressure) due to the relation between $P_v(t=0)$ and P_0 via homogeneous nucleation theory (2), and the static equilibrium of the initial bubble (i.e. $\Delta P_i \approx 2\sigma/r$ where σ is surface tension and r is the initial bubble radius) as shown in figure 9. The pressure difference which drives isothermal growth will then diminish, and so will the growth rate, as P_0 increases. The variation of ΔP_i with P_0 is responsible for the existence of a threshold pressure above which explosive vaporization will not occur for a fluid of fixed composition.

For thermally limited (i.e. isobaric) growth, $P_v(t) \to P_0$ at which time the temperature difference for thermal energy transport reaches a maximum,

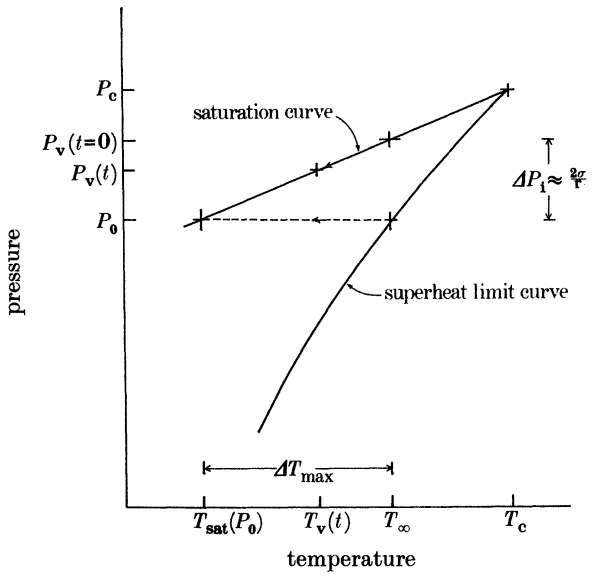

FIGURE 9. Schematic variation of initial excess bubble pressure, ΔP_i, and maximum temperature difference, ΔT_{max}, with P_0 for a fluid of fixed composition on a P–T diagram (cf. figure 4). Arrows indicate the direction of change of $T_v(t)$ and $P_v(t)$ during growth of a bubble.

$\Delta T_{max} \equiv T_\infty - T_{sat}(P_0)$ where $T_{sat}(P_0)$ is the saturation temperature corresponding to P_0. This maximum temperature difference is related to ΔP_i through the variation of T_∞ with P_0 given by homogeneous nucleation theory (e.g. (2)), and $T_{sat}(P_0)$ to P_0 and $P_v(t=0)$ to T_∞ provided by equilibrium saturation relations. In particular, as $P_0 \to P_c$, $\Delta T_{max} \to 0$ so that the thermally limited growth rate will decrease. This decrease with increasing ambient pressure was observed in the present experiments as noted above; the reported data were obtained at times during which bubble growth was believed to be heat transfer controlled (based on reference to a complete analysis for a simplifed geometry by Avedisian & Suresh (1985)).

The effect of liquid composition on the droplet expansion rate is shown in figures 10 & 11. Figure 10 presents data for two binary mixtures and one ternary mixture at an approximately constant pressure of 0.75 MPa. The variation in initial droplet (i.e. nucleation) temperature shown in table 1 reflects a composition dependence on the limit of superheat. For these mixtures the concentration of pentane was fixed at 80 % and the composition of the remaining 20 % consisted of either pure hexane, pure decane (for the binary mixtures), or a mixture of hexane and decane (thus forming a ternary mixture).

Replacing hexane with decane in the binary system reduced the droplet expansion (i.e. bubble growth) rate. However, replacing part, but not all, of the 20 % hexane in the binary pentane–hexane mixture with decane to form a ternary pentane–hexane–decane mixture nearly *doubled* the rate of vaporization above that of either the pentane–hexane or pentane–decane mixtures. This result is interesting in that it shows that for the system studied dilution of a binary mixture by a third non-volatile component, thus forming a ternary mixture, can *increase*

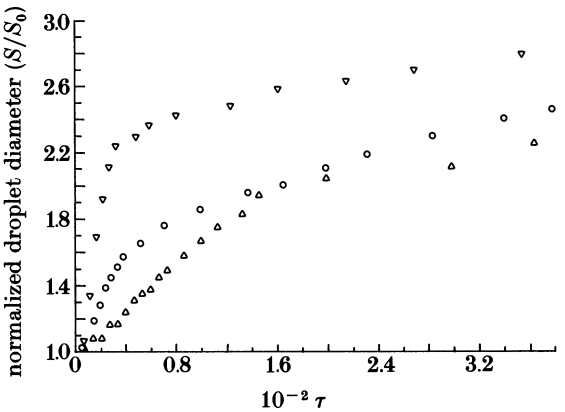

FIGURE 10. Variation of droplet diameter with time at constant pressure for three mixtures at 0.75(±0.04) MPa. ○, pentane–hexane ($0.8C_5:0.2C_6$); △, pentane–decane ($0.8C_5:0.2C_{10}$); ▽, pentane–hexane–decane ($0.8C_5:0.1C_6:0.1C_{10}$). Pentane concentration is fixed at 80 %.

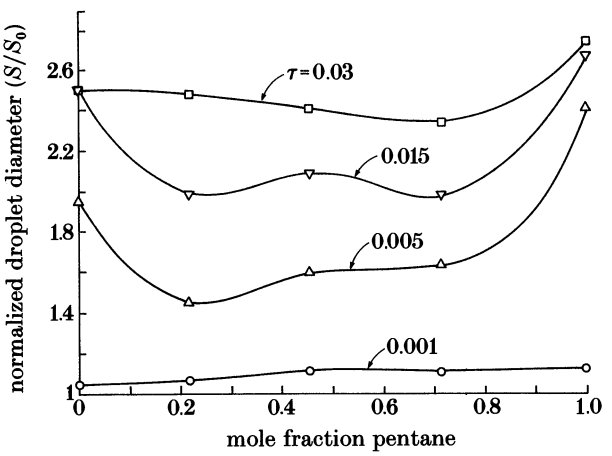

FIGURE 11. Effect of composition on droplet diameter at the indicated times for a binary pentane–hexane mixture. Solid line drawn through the data is a curve of best fit.

the growth rate above that of a binary mixture with the composition of the most volatile component fixed (i.e. pentane in the present experiments). The generalization of this result requires further experiments. The expectation was that the growth rate of the pentane–hexane–decane mixture would be intermediate to the pentane–hexane and pentane–decane mixtures. The reason for the substantial increase in the expansion rate of the ternary mixture as shown in figure 10 could be due to a peculiar effect of composition on the ternary liquid diffusion coefficient, but no such data are available.

Figure 11 shows the effect of composition in a binary pentane–hexane mixture on droplet diameter at various times τ during vaporization. The pressure is approximately constant (0.77 MPa) and the lines through the data are curves of

best fit to more clearly illustrate the variation. Diluting hexane by pentane was found to *lower* the droplet vaporization rate compared to vaporization of a pure hexane droplet at the homogeneous nucleation limit. This reduction persists throughout growth except apparently at the earliest periods ($\tau < 0.001$), at which times dilution of hexane by pentane results in the droplet expanding *faster* for the binary mixture than in pure hexane. At later times, a droplet expands faster for the mixture than for pure hexane only when hexane is diluted by over 90% pentane. This reduction in growth rate for a binary mixture is not without precedent. For a binary mixture of *infinite* extent containing a vapour bubble growing within it, bubbles have been predicted to grow slower within the mixture than within its components, the reason being due to the resistance to mass diffusion of the volatile component within the mixture to the bubble wall (Scriven 1959).

An analysis of non-explosive bubble (and droplet) growth within a multicomponent liquid droplet at its superheat limit has not been presented, except for a single component liquid droplet (Avedisian & Suresh 1985). Information from previous results for a stationary vapour bubble growing in an *unbounded* quiescent binary liquid (a droplet of infinite radius) may, however, be used as a basis for understanding qualitative characteristics of the vaporization rates of droplets during periods in which both the mass diffusion and thermal boundary layers remain within the droplet boundary, and effects of motion of the field liquid exert a negligible influence on the flow and heat transfer within the droplet (i.e. for a 'slowly' moving ambient fluid such that $Pe \ll Ja^3$ where Ja is the mixture Jakob number). For this purpose it is most convenient to consider the simplest bubble–droplet geometry, a vapour bubble growing from the centre of a liquid droplet. Because $\alpha/D \sim 10$ (D is the mass diffusion coefficient) for the mixtures studied, the mass diffusion boundary layer is thinner than the thermal boundary layer. In view of the fact that the thermal boundary layer should, for a concentric bubble–droplet system, reside within the droplet during some initial period of growth, with the specific time period depending on the mixture properties and ambient conditions, an infinite medium analysis could then conceivably be applicable during this initial period.

Scriven (1959) and Skinner & Bankoff (1964) derived the growth law for a vapour bubble within a stationary infinite binary mixture in the form

$$d/S_0 = 4\beta\sqrt{\tau}. \tag{4}$$

The growth constant, β, is a function of bulk liquid composition (x_∞), the local composition at the bubble wall (x_b), and vapour temperature T_∞ ($\neq T_{sat}$ due to preferential vaporization of the volatile component). In the general case it can only be determined numerically, and none of the often quoted limiting analytical expressions for β derived by Scriven (1959) were found to be valid for conditions of the experiments reported here. β was, therefore, determined numerically in the present work. Because S rather than d was measured in our experiments (4) for a spherical bubble–droplet system can be written as

$$S/S_0 = [1 + \epsilon\,(4\beta\tau^{\frac{1}{2}})^3]^{\frac{1}{3}}. \tag{5}$$

Figure 12 compares predicted droplet diameters (by using property estimation

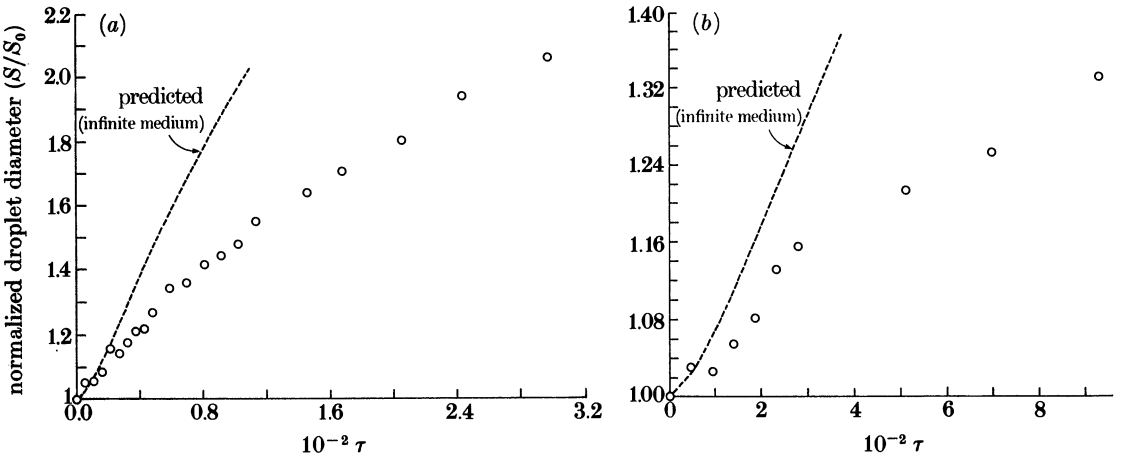

FIGURE 12. Comparison between calculated (line) and measured (circles) droplet diameters. Calculation is based on the Scriven (1959) infinite medium analysis. (*a*) $0.22C_5{:}0.78C_6$, $P_0 = 1.04$ MPa, drop 7; (*b*) $0.46C_5{:}0.54C_6$, $P_0 = 1.18$ MPa, drop 14.

techniques for mixtures given in Reid *et al.* (1977)) with measured values for two representative pentane–hexane mixtures at 1.08 and 1.18 MPa. The agreement is qualitative at early times and deviates significantly at progressively later times, with the droplet growing at a much slower rate than predicted. This behaviour reflects the fact that at later times the thermal and mass diffusion boundary layers penetrate into the field liquid with a concomitant influence of the field liquid on the temperature distribution within the droplet and heat-transfer rate to the internal bubble, so that the infinite medium analysis is inapplicable at these later times. In addition, the assumed bubble–droplet geometry may not be quite right in that the bubble within the droplet may be eccentrically positioned. If the bubble grows at the liquid–liquid boundary, the droplet expansion rate could be reduced (or increased) earlier in the vaporization process, depending on the field-liquid properties (Avedisian & Suresh 1985). We also note that the calculation of β was rather sensitive to the choice of physical property correlations. All liquid properties were evaluated at the mean temperature between the bubble and ambient, and mixture heat of vaporization and vapour properties were evaluated at $T_{\mathrm{sat}}(P_0)$.

4. Conclusions

The present experiments illustrated the following facts for vaporization of a superheated multicomponent liquid droplet at the homogeneous nucleation limit.

1. A droplet consisting of a pure non-volatile liquid generally evaporates faster than one that is a binary mixture unless the non-volatile liquid is substantially diluted by the volatile liquid.

2. A droplet was found to vaporize faster for a ternary pentane–hexane–decane mixture than for binary pentane–hexane or pentane–decane mixtures. The generalization of this result, however, requires further experiments.

3. The droplet expansion rate for a multicomponent droplet always decreases as pressure increases.

4. An analysis for vapour bubble growth within a mixture of infinite extent is not generally applicable to bubbles growing within droplets.

The laboratory assistance of Mr Matthew Krane is appreciated. Conversations with Professor T. K. Nguyen of California State Polytechnic University, Pomona and Professor C. H. Wang of National Taiwan University have been helpful. The photographic equipment was purchased with support received from the National Science Foundation under grant no. CBT-8305263 and CBT-8451075. This work formed part of a project supported by the U.S. Department of Energy under contract no. DE-ACO2-83ER13092 from the Office of Basic Energy Sciences – Engineering Research Program with Dr Oscar P. Manley as Project Monitor.

References

Apfel, R. E. & Harbison, J. P. 1975 *J. acoust. Soc. Am.* **57** (60), 1371–1373.
Avedisian, C. T. 1982 *J. Heat Transfer* **104**, 750–757.
Avedisian, C. T. & Sullivan, J. R. 1984 *Chem. Engng Sci.* **39** (6), 1033–1041.
Avedisian, C. T. & Suresh, K. 1985 *Chem. Engng Sci.* **40** (12), 2249–2259.
Blander, M., Hengstenberg, D. & Katz, J. L. 1971 *J. phys. Chem.* **75**, 3613–3619.
Frost, D. & Sturtevant, B. 1986 *J. Heat Transfer* **108**, 418–424.
Mori, Y. H. & Komotori, K. 1976 *Heat Transfer, Jap. Res.* **5**, 75–95.
Reid, R. C., Prausnitz, J. M. & Sherwood, T. K. 1977 *Properties of gases and liquids*, 3rd edn. New York: McGraw-Hill
Scriven, L. E. 1959 *Chem. Engng Sci.* **10**, 1–13.
Shepherd, J. & Sturtevant, B. 1982 *J. Fluid Mech.* **121**, 379–402.
Skinner, L. A. & Bankoff, S. G. 1964 *Physics Fluids.* **7**, 643–648.

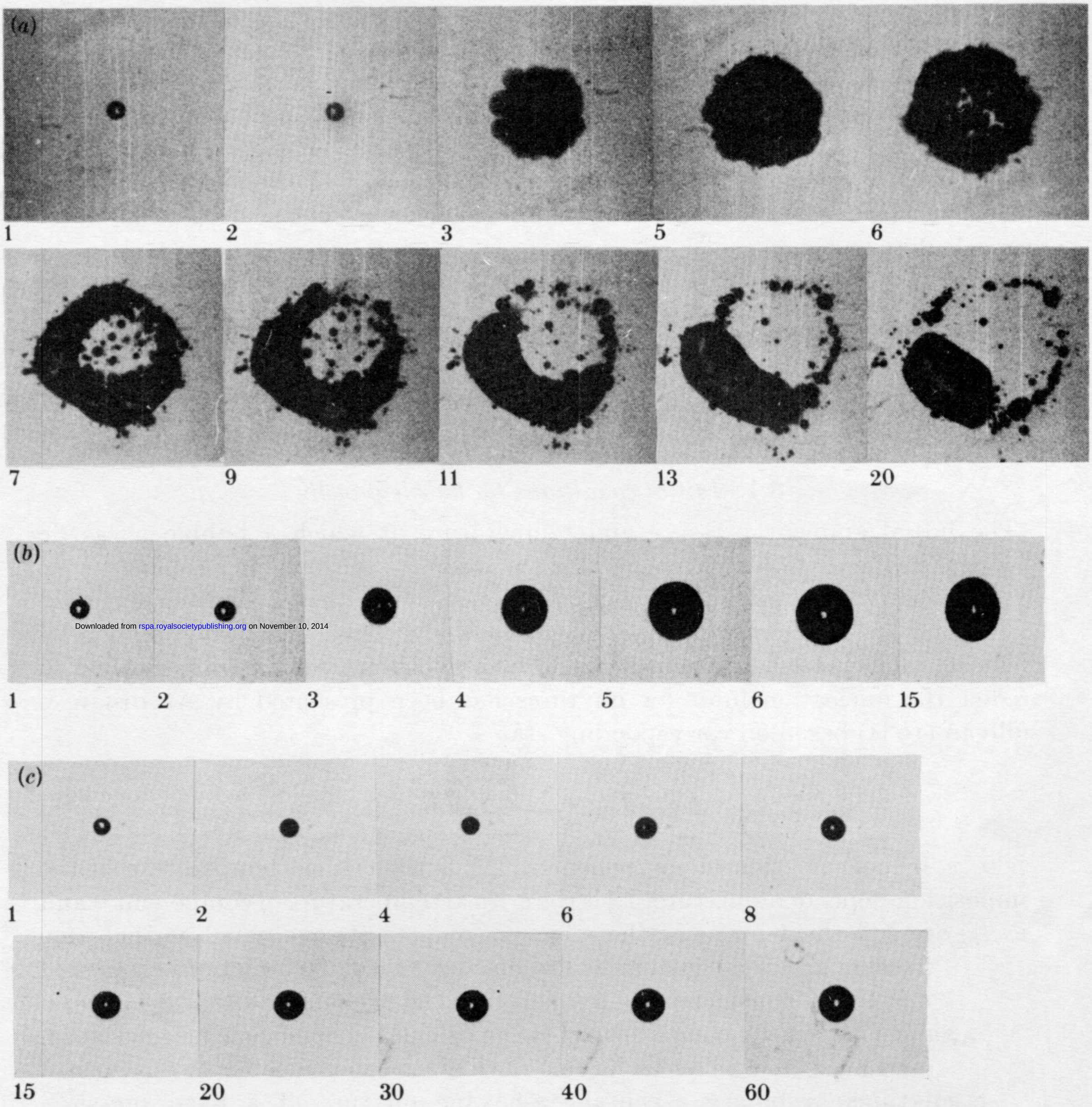

FIGURE 2. Levitated droplets at their superheat limits in glycerine. Flow is from left to right. Number on each picture corresponds to the position in the motion picture sequence. (*a*) *n*-hexane: $P_0 = 0.12$ MPa, $T_\infty = 460$ K, $S_0 = 0.72$ mm, frames $s^{-1} = 900$; (*b*) *n*-hexane: $P_0 = 0.44$ MPa, $T_\infty = 461.3$ K, $S_0 = 0.76$ mm, frames $s^{-1} = 500$; (*c*) *n*-pentane (0.715)–*n*-hexane (0.285) mixture: $P_0 = 0.93$ MPa, $T_\infty = 450$ K, $S_0 = 0.7$ mm, frames $s^{-1} = 500$. White dot in droplet centre is light reflection.